

Rotational tuning of H_{c2} anomalies in $\text{ErNi}_2\text{B}_2\text{C}$: Angular-dependent superzone gap formation and its effect on the superconducting ground state

Sergey L. Bud'ko and Paul C. Canfield

Ames Laboratory and Department of Physics and Astronomy, Iowa State University, Ames, Iowa 50011

(Received 22 February 2000)

$\text{ErNi}_2\text{B}_2\text{C}$ is a member of the $R\text{Ni}_2\text{B}_2\text{C}$ family of magnetic superconductors, with $T_c \approx 11$ K and $T_N \approx 6$ K. For magnetic fields applied along the magnetically hard c axis, the upper critical field H_{c2} manifests a clear, sharp local maximum at T_N . For magnetic fields applied within the basal plane, features in H_{c2} are less distinct and there are field induced changes in the local magnetic ordering. In order to address the relationship between H_{c2} and local moment order, anisotropic magnetic and transport measurements on single crystals of $\text{ErNi}_2\text{B}_2\text{C}$ will be presented. In particular, detailed H - T phase diagrams for different orientations of the applied field, as well as possible evidence of a superzone gap formation at the antiferromagnetic phase transition and its effect on anisotropic upper critical field, will be discussed. The anomaly in H_{c2} as well as sharp features in the normal-state resistivity can be tuned by changing the orientation of the applied field. This is consistent with tuning in and out of the $0.55a^*$ magnetically ordered, superzone gapped phase.

Local moment magnetic order and superconductivity have conventionally been considered as antagonistic ground states. The first examples of coexistence of these two ground states were found in the late 1970s in $RRh_4\text{B}_4$ and $R\text{Mo}_6(\text{S}/\text{Se})_6$ (R =rare earth).¹ These materials attracted a great deal of theoretical and experimental attention. By the 1980s a large body of theoretical understanding of the coexistence of superconductivity and long-range magnetic order had emerged, but experiments were mainly performed on polycrystalline materials, in which the averaging of properties over the individual crystallites prevented addressing any issues of anisotropy. The recently discovered^{2,3} family of quaternary borocarbides $R\text{Ni}_2\text{B}_2\text{C}$ gives several exciting examples of coexistence of antiferromagnetism and superconductivity with the ratio of the superconducting ordering temperature to the Néel temperature T_c/T_N varying from 7.3 to 0.6 (Ref. 4) with both T_c and T_N easily accessible in experiment. In addition, a few months after the discovery these materials were grown in a single crystalline form.

The particular case of $\text{ErNi}_2\text{B}_2\text{C}$ appears to be of specific interest. Superconductivity ($T_c \approx 11$ K) in this compound coexists with the antiferromagnetically ordered state below $T_N \approx 6$ K, and the in-plane superconducting critical field differs from the c -axis one, both in magnitude and temperature dependence near T_N .⁵ In addition, at lower temperatures ($T_{WF} \approx 2.5$ K) "weak ferromagnetism" (ordered state with a net ferromagnetic component to the ordered moment) was suggested (based on magnetization and heat-capacity measurements) to coexist with superconductivity.⁶ Recent neutron-diffraction data⁷ confirmed this initial speculation, and critical currents were found⁸ to be strongly enhanced for all orientations of the applied field in this "weak ferromagnetic" regime, corresponding to an increase of the pinning force of the flux-line lattice. A possibility of formation of the spontaneous vortex lattice below T_{WF} in $\text{ErNi}_2\text{B}_2\text{C}$ was suggested.⁹

In this paper we will examine the anisotropy of the upper superconducting critical field H_{c2} in detail. Earlier studies^{4,5}

found that there was a significant anisotropy in the temperature dependence of H_{c2} . Specifically, there was a sharp cusp in H_{c2} for $H \parallel c$ and merely an inflection for $H \perp c$. Whereas the $H \parallel c$ data are consistent with magnetic ordering with a wave vector of $0.55a^*$ (Refs. 4, 5, 10, and 11), the $H \perp c$ data give rise to the question, why is there no cusp in H_{c2} for the magnetic field applied in the basal plane? In order to answer this question we will present the results of detailed, anisotropic magnetization and transport measurements on $\text{ErNi}_2\text{B}_2\text{C}$ single crystals. Anisotropic H - T phase diagrams for the three unique crystallographic directions: $[100]$, $[110]$, and $[001]$, clearly show that $\text{ErNi}_2\text{B}_2\text{C}$ is a system that can be tuned in and out of a specific magnetically ordered state that causes the sharp suppression of H_{c2} just below T_N .

Single crystals of $\text{ErNi}_2\text{B}_2\text{C}$ were grown using the Ni_2B flux growth technique.^{4,5,12} After the crystals were cut into oriented bars they were annealed in vacuum at 900°C for 30 h so as to further reduce internal strains and cause a slight increase of H_{c2} and a decrease of the superconducting transition width. Magnetization measurements were made using a Quantum Design MPMS-5 superconducting quantum interference device (SQUID) magnetometer. Magnetoresistance was measured by standard four-probe technique with the current flowing along $[100]$ or $[110]$ axis of the sample using LR-400 ac resistance bridge and the H - T environment of MPMS-5. Measurements were repeated on single crystals from several different batches. H_{c2} curves were obtained from the temperature and field-dependent resistance measurements in a manner similar to that described in Ref. 5. The sharpness and the position of the anomalies in the $H_{c2}(T)$ curves does not depend on the criterion used in a definition of T_c obtained from $\rho(T, H)$ measurements (Fig. 1). The R_0 criterion (see inset to Fig. 1) was used for $H_{c2}(T)$ curves presented in Fig. 2 and Fig. 3. Although the absolute value of H_{c2} at a given temperature varies slightly from sample to sample, the features in $H_{c2}(T)$ curves for different orientations of the applied field are very robust and reproducible, the position of the different magnetic phase bound-

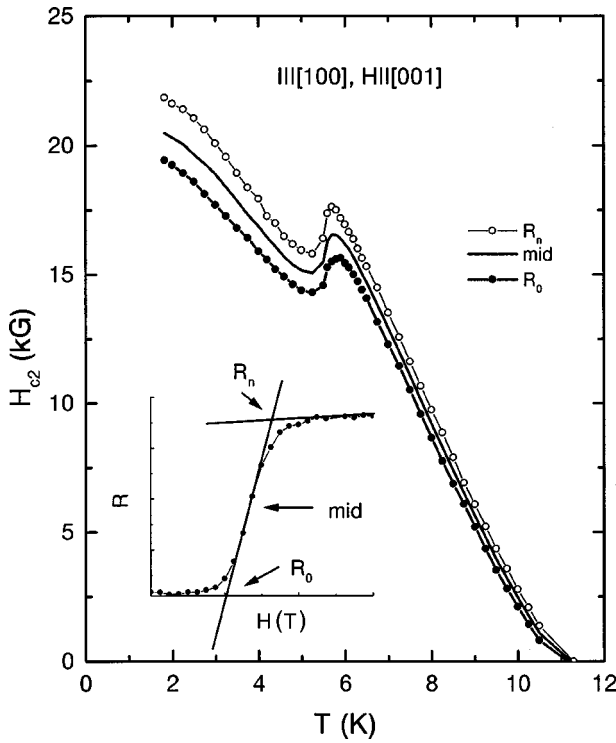


FIG. 1. Upper critical field of $\text{ErNi}_2\text{B}_2\text{C}$ for $H\parallel[001]$ obtained from $\rho(T, H)$ measurements using different criteria.

aries (see below) are practically sample independent as well. The magnetic phase boundaries (Fig. 3) were drawn based on field and temperature-dependent magnetization measurements. The specific data points were determined in the same way as it was done for $\text{HoNi}_2\text{B}_2\text{C}$.^{13,14}

The temperature dependencies of the superconducting critical field H_{c2} in $\text{ErNi}_2\text{B}_2\text{C}$ for three high symmetry orientations are shown in Fig. 2. Noticeable anisotropy in H_{c2}

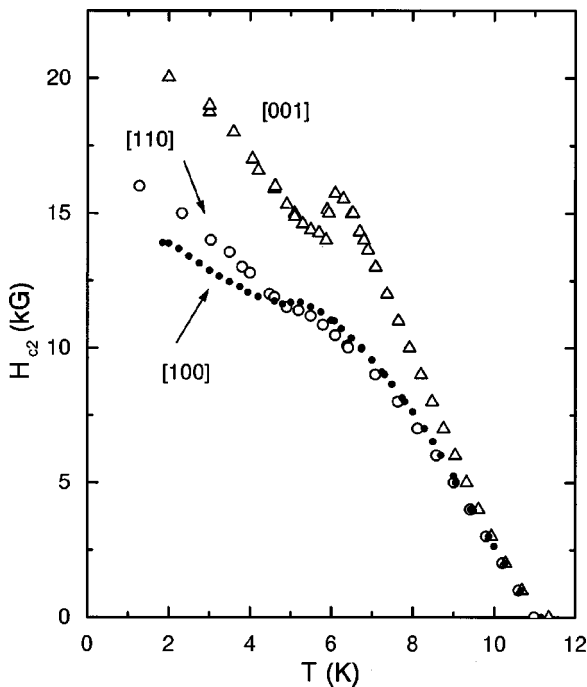


FIG. 2. Anisotropic upper critical field of $\text{ErNi}_2\text{B}_2\text{C}$.

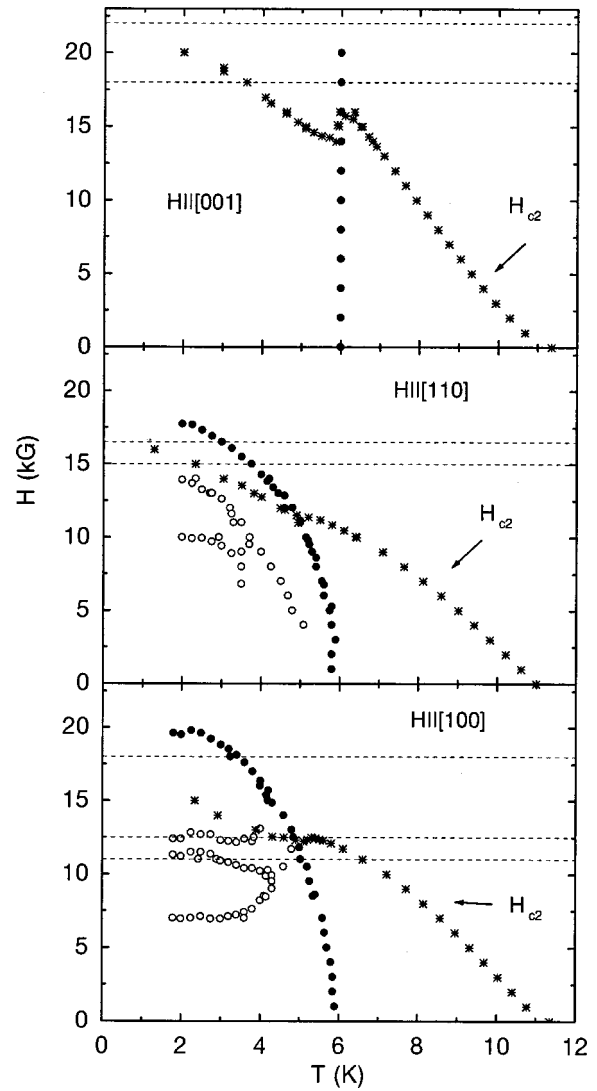


FIG. 3. H - T phase diagrams for $\text{ErNi}_2\text{B}_2\text{C}$. symbols: * - H_{c2} , closed circles - T_N , open circles - phase lines separating different types of local magnetic order. Horizontal lines mark fields at which $\rho(T)$ data in Fig. 4 were taken.

is observed not only between in-plane and perpendicular to the ab plane⁵ but also for the $[100]$ and $[110]$ directions of the applied field. The difference in magnitude of H_{c2} (2 K) is consistent with the anisotropic magnetization M_{100} (2 K) $>$ M_{110} (2 K) $>$ M_{001} (2 K) of the Er sublattice.^{5,14,15} The decrease of H_{c2} just below T_N is sharp for $H\parallel[001]$, less pronounced for $H\parallel[100]$ and it vanishes for $H\parallel[110]$ (Fig. 2). Theoretical explanations for a similar sharp feature in H_{c2} at T_N observed in ternary magnetic superconductors were given by Machida *et al.*¹⁰ and by Ramakrishnan and Varma.¹¹ Although these two groups used different theoretical approaches, in both cases the crucial prerequisite for a sharp local maximum in H_{c2} at T_N was that the wave vector associated with the magnetically ordered state is determined by a Fermi-surface nesting. The sharp anomaly in H_{c2} at T_N for $H\parallel c$ in $\text{ErNi}_2\text{B}_2\text{C}$ can be explained⁵ in a similar way. Indeed, band-structure calculations¹⁶ suggest Fermi-surface nesting in the borocarbides (recently observed in $\text{LuNi}_2\text{B}_2\text{C}$ by electron-positron annihilation technique¹⁷) leading to a maximum in the generalized susceptibility $\chi(q)$ for the wave vec-

tor $q \approx (0.6, 0, 0)$, and the neutron-diffraction measurements on $\text{ErNi}_2\text{B}_2\text{C}$ in magnetically ordered state in zero applied field^{18,19} reveal an incommensurate antiferromagnetic structure with the wave vector $0.55a^*$. Two possible explanations were suggested^{4,5} for observed smearing of the anomaly in H_{c2} near T_N for $H \perp c$: the first is that, while T_N is independent of the applied field for $H \parallel c$, for $H \perp c$ it decreases with field, which causes broadening of the feature in H_{c2} ; the second possibility is that for some $H < H_{c2}$ there is a change in the ordering wave vector, so that it differs from the nesting wave vector and therefore does not meet the criterion in Refs. 10 and 11.

To address this point, detailed composite magnetic and superconducting H - T phase diagrams (Fig. 3) for $H \parallel [100]$, $H \parallel [110]$, and $H \parallel [001]$ were constructed based on $M(H, T)$ and $\rho(H, T)$ measurements as described above. For $H \parallel [001]$ there is only one, vertical line in the magnetic phase diagram. Based on our knowledge of the zero-field state^{18,19} we assume that the whole measured H - T region to the left of this line is associated with the $0.55a^*$ state and therefore when the $H_{c2}(T)$ curve penetrates into the magnetically ordered region it enters the $0.55a^*$ state. In this case, as mentioned above, there is a clear cusp in $H_{c2}(T)$. For $H \parallel [100]$ the $H_{c2}(T)$ curve penetrates the magnetically ordered state at the point where the H - T area associated with the $0.55a^*$ phase is disappearing. For $H \parallel [100]$ there is a clear, but smaller cusp in H_{c2} (Fig. 2 and Fig. 3). For $H \parallel [110]$ the $H_{c2}(T)$ penetrates into the magnetically ordered state in an area that is distinct from the $0.55a^*$ area and there is no discernible local maximum in the $H_{c2}(T)$ curve. So far, the results support the models based on the Fermi-surface nesting^{10,11} if we infer, that the ordering wave vector changes from one ordered phase to another when a magnetic phase boundary is crossed. In this case for $H \parallel [110]$ the magnetic ordering wave vector no longer coincides with the nesting wave vector and $H_{c2}(T)$ has no local maximum. For $H \parallel [100]$ an intermediate case occurs due to the proximity of the superconductivity-magnetic order crossing point in H - T phase diagram to the phase boundary between the low-field $0.55a^*$ ordering and higher field metamagnetic phase. In essence then $\text{ErNi}_2\text{B}_2\text{C}$ can be tuned in and out in compliance with Machida/Ramakrishnan-Varma criterion by simply changing the direction of the applied magnetic field.

To further test this idea of ‘‘tunability’’ in the case of $\text{ErNi}_2\text{B}_2\text{C}$ we examined $\rho(H, T)$ data for $T \sim T_N(H)$. If the above premises are correct we anticipate seeing a signature of the superzone gap at $T_N(H)$ in transport properties for some, but not all, directions of applied field.²⁰ An applied field is required because the magnetically ordered state must be entered with the sample in the normal (nonsuperconducting) state. In order to expose more of the magnetic phase diagram a sample with a slightly lower $H_{c2}(T)$ curve than that shown in Figs. 2 and 3 was used. The temperature-dependent resistivity of $\text{ErNi}_2\text{B}_2\text{C}$ for $I \parallel [100]$ and different directions of applied field is plotted in Fig. 4. For $H \parallel [001]$ and $H \parallel [110]$ the resistivity measurements are certainly consistent with the aforementioned application of the Fermi-surface nesting based models to $\text{ErNi}_2\text{B}_2\text{C}$. For $H \parallel [001]$ there is an upturn in $\rho(T)$ near T_N which is a signature of the antiferromagnetic superzone gap formation (with the size of the anomaly being comparable with the estimate of the frac-

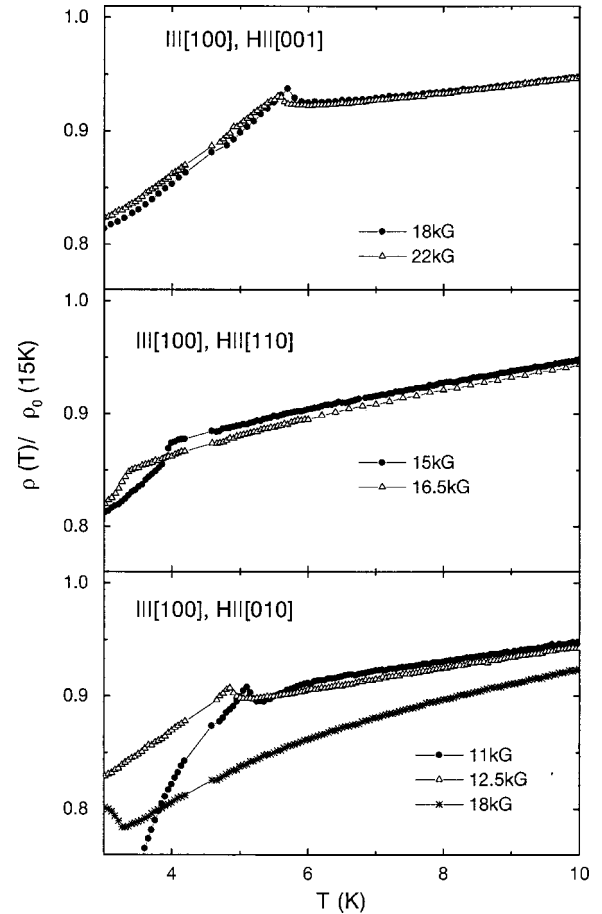


FIG. 4. Normalized resistivity of $\text{ErNi}_2\text{B}_2\text{C}$ in applied magnetic field.

tion of the Fermi surface participating in the nesting¹⁷). For $H \parallel [110]$ there is no upturn in $\rho(T)$, consistent with a lack of nesting in this state. For $H \parallel [100]$ the situation is a little more complex but appears to be consistent with the other data. For fields of 11 kG and 12.5 kG applied along the $[100]$ direction $\text{ErNi}_2\text{B}_2\text{C}$ initially orders with the $0.55a^*$ wave vector (see Fig. 3) and manifests a superzone gap feature similar to that seen for $H \parallel [001]$. For higher applied fields (18 kG) $\text{ErNi}_2\text{B}_2\text{C}$ enters in a part of the H - T phase diagram associated with a different, metamagnetic state. The feature in the 18 kG resistivity curve is of a different nature and would require detailed information about the metamagnetic state to analyze.

Whereas these resistivity data support our hypothesis that $\text{ErNi}_2\text{B}_2\text{C}$ can be tuned in and out of a superzone-gapped state, it should be noted that unlike the features in H_{c2} and the H - T phase diagrams, the relatively small upturn in the resistivity that is the hallmark of the superzone gap in the transport measurements is a rather fragile feature and was observed in only about half of the samples. We do not feel that this represents a fundamental error in our hypothesis, but rather illustrates how difficult it is to observe superzone gaps via transport measurements.

Summing up, detailed magnetization and transport measurements on $\text{ErNi}_2\text{B}_2\text{C}$ give evidence that this material presents a remarkably clear example of being able to tune the magnetic and superconducting properties by changing the orientation and magnitude of the applied magnetic field. We

find a strong correlation between the local maximum in H_{c2} and the nature of the magnetically ordered state: when $H_{c2}(T)$ penetrates into the magnetically ordered part of the H - T phase diagram that has $0.55a^*$ order and that manifests a superzone gap in the normal-state resistivity, then there is a sharp local maximum in H_{c2} . When $H_{c2}(T)$ penetrates into a part of the H - T phase diagram that has a different type of magnetic order, then there is no local maximum in $H_{c2}(T)$. These experimental observations are fully consistent with

theories by Machida *et al.*¹⁰ and Ramakrishnan and Varma¹¹ which incorporate Fermi-surface nesting features.

We thank K. O. Cheon for help in sample preparation and initial measurements and P. L. Gammel for enlightening discussions. Ames Laboratory is operated for the U.S. Department of Energy by Iowa State University under Contract No. W-7405-Eng-82. This work was supported by the Director for Energy Research, Office of Basic Energy Sciences.

-
- ¹For a review, see Ø. Fisher, in *Ferromagnetic Materials*, edited by K. H. J. Buschow and E. P. Wolfarth (North Holland, Amsterdam, 1990), Vol. 5, p. 465.
- ²R. Nagarajan, C. Mazumdar, Z. Hossain, S. K. Dhar, K. V. Gopalakrishnan, L. C. Gupta, C. Godart, B. D. Padalia, and R. Vijayaraghavan, *Phys. Rev. Lett.* **72**, 274 (1994).
- ³R. J. Cava, H. Takagi, H. W. Zandbergen, J. J. Krajewski, W. F. Peck, Jr., T. Siegrist, B. Battlog, R. B. van Dover, R. J. Felder, K. Mizuhashi, J. O. Lee, H. Eisaki, and S. Uchida, *Nature (London)* **376**, 252 (1994).
- ⁴P. C. Canfield, P. L. Gammel, and D. J. Bishop, *Phys. Today* **51** (10), 40 (1998), and references therein.
- ⁵B. K. Cho, P. C. Canfield, L. L. Miller, D. C. Johnston, W. P. Beyermann, and A. Yatskar, *Phys. Rev. B* **52**, 3684 (1995).
- ⁶P. C. Canfield, S. L. Bud'ko, and B. K. Cho, *Physica C* **262**, 249 (1996).
- ⁷H. Kawano, H. Takeya, H. Yoshizawa, and K. Kadowaki, *J. Phys. Chem. Solids* **60**, 1053 (1999).
- ⁸P. L. Gammel, B. Barber, D. Lopez, A. P. Ramirez, D. J. Bishop, S. L. Bud'ko, and P. C. Canfield, *Phys. Rev. Lett.* **84**, 2497 (2000).
- ⁹T. K. Ng and C. M. Varma, *Phys. Rev. Lett.* **78**, 3745 (1997).
- ¹⁰K. Machida, K. Nokura, and T. Matsubara, *Phys. Rev. B* **22**, 2307 (1980).
- ¹¹T. V. Ramakrishnan and C. M. Varma, *Phys. Rev. B* **24**, 137 (1981).
- ¹²M. Xu, P. C. Canfield, J. E. Ostenson, D. K. Finnemore, B. K. Cho, Z. R. Wang, and D. C. Johnston, *Physica C* **227**, 321 (1994).
- ¹³P. C. Canfield, S. L. Bud'ko, B. K. Cho, A. Lacerda, D. Farrell, E. Johnston-Halperin, V. A. Kalatsky, and V. L. Pokrovsky, *Phys. Rev. B* **55**, 970 (1997).
- ¹⁴P. C. Canfield and S. L. Bud'ko, *J. Alloys Compd.* **262-263**, 169 (1997).
- ¹⁵For a review, see Ø. Fisher, M. Ishikawa, M. Pelizzone, and A. Treyvaud, *J. Phys. (Paris), Colloq.* **40**, C5-89 (1979).
- ¹⁶J. Y. Rhee, X. Wang, and B. N. Harmon, *Phys. Rev. B* **51**, 15 585 (1995).
- ¹⁷S. B. Dugdale, M. A. Alam, I. Wilkinson, R. J. Hughes, I. R. Fisher, P. C. Canfield, T. Jarlborg, and G. Santi, *Phys. Rev. Lett.* **83**, 4824 (1999).
- ¹⁸J. Zarestky, C. Stassis, A. I. Goldman, P. C. Canfield, P. Dervenagas, B. K. Cho, and D. C. Johnston, *Phys. Rev. B* **51**, 678 (1995).
- ¹⁹S. K. Sinha, J. W. Lynn, T. E. Grigereit, Z. Hossain, L. C. Gupta, R. Nagarajan, and C. Godart, *Phys. Rev. B* **51**, 681 (1995).
- ²⁰H. Miwa, *Prog. Theor. Phys.* **29**, 477 (1963).